$K\alpha$ satellite transition assignments for medium-Z elements

William J. Kuhn and Bruce L. Scott
Department of Physics-Astronomy, California State University, Long Beach, Long Beach, California 90840
(Received 21 January 1986)

Nonrelativistic Hartree-Fock calculations have been used in intermediate coupling to calculate transition energies and relative intensities for $K\alpha$ satellites for all elements from K ($Z=19$) through Ge ($Z=32$). It is found that the $2s$ spectator-hole transitions $(1s\,2s)^{-1}\rightarrow(2s\,2p)^{-1}$ contribute negligibly, whereas all satellites except α'' can be assigned to allowed transitions from the $(1s\,2p)^{-1}\rightarrow(2p)^{-2}$ complex.

I. INTRODUCTION

$K\alpha$ x-ray satellite lines[1] have been known for many years and a general understanding of their origin has been given. Druyvesteyn[2] first suggested the accepted explanation—the near satellites are caused by transitions involving a spectator hole in the L shell: $(1s\,2s)^{-1}\rightarrow(2s\,2p)^{-1}$ and $(1s\,2p)^{-1}\rightarrow(2p)^{-2}$. Kennard and Ramberg[3] made self-consistent-field calculations in intermediate coupling with results only roughly agreeing with the available experimental data. More recent calculations have been made by Gianturco, Semprini, and Stefani,[4] Sachenko and Demekhin,[5] and Horák.[6] Although all of these calculations support the hypothesis of Druyvesteyn, none can be considered definitive in establishing a definite correspondence between the theoretical transition spectrum and experimental results. The probable reason for this is that all of the aforementioned calculations were made before the easy availability of fast reliable computers and programs for solving the Hartree-Fock equations.

More recently, Nigam and Kothari[7] reexamined the satellites of iron and used the calculations of Gianturco, Semprini, and Stefani[4] to establish correspondences. In particular, they proposed that the weak α_3'' satellite was due to a transition forbidden in Russell-Saunders coupling but allowed in the intermediate-coupling scheme. This conclusion seems questionable so the entire problem has been reexamined using the modern computational facilities available to us.

II. CALCULATIONS

All calculations were done in intermediate coupling using nonrelativistic Hartree-Fock energies, Slater integrals, and spin-orbit parameters calculated by the FORTRAN code of Froese Fischer.[8] Only single configurations were used and only the two-hole transitions $(1s\,2s)^{-1}\rightarrow(2s\,2p)^{-1}$ and $(1s\,2p)^{-1}\rightarrow(2p)^{-2}$ were considered.

It is well known that Hartree-Fock energies for states involving $1s$ holes are greatly in error. In order to correct for this we calculated the difference in energy between a given transition and the $K\alpha$ average energy and added the experimental average $K\alpha$ energies to obtain our "theoretical" results:

$$E=E(1s^{-1}2s^{-1})-E(2s^{-1}2p^{-1}) \tag{1a}$$

$$=E(1s^{-1}2s^{-1})-E(2s^{-1}2p^{-1})-[E(1s^{-1})-E(2p^{-1})]+[E(1s^{-1})-E(2p^{-1})]$$

$$=E(1s^{-1}2s^{-1})-E(2s^{-1}2p^{-1})-E(1s^{-1})+E(2p^{-1})+E(K\alpha)_{\rm av}\ . \tag{1b}$$

In Eq. (1b) the average $K\alpha$ energy $E(K\alpha)_{\rm av}$ is computed by

$$E(K\alpha)_{\rm av}=[2E(K\alpha_1)+E(K\alpha_2)]/3\ . \tag{2}$$

The first four terms in Eq. (1b) were computed from the Hartree-Fock code while Eq. (2) was evaluated using the tabulated energies of Bearden and Burr.[9] The spin-orbit parameter $\zeta_{\rm eff}$ was determined by normalizing the

TABLE I. Hamiltonian matrix in L-S coupling. The configurations $(1s\,2s)$, $(1s\,2p^5)$, $(2s\,2p^5)$, and $(2p^4)$ are given. G^0, G^1, and F^2 are the usual Slater integrals, while ζ is the spin-orbit parameter. (a) $(1s\,2s)$, (b) $(1s\,2p^5)$ and $(2s\,2p^5)$, (c) $2p^4$.

(a)

	$^1S_0$	$^3S_1$
$^1S_0$	$E_0+3G^0/2$	0
$^3S_1$	0	$E_0-G^0/2$

(b)

	$^1P_1$	$^3P_1$	$^3P_0$	$^3P_2$
$^1P_1$	$E_0+G^1/2$	$\zeta/\sqrt{2}$	0	0
$^3P_1$	$\zeta/\sqrt{2}$	$E_0-G^1/6+\zeta/2$	0	0
$^3P_0$	0	0	$E_0-G^1/6+\zeta$	0
$^3P_2$	0	0	0	$E_0-G^1/6-\zeta/2$

(c)

	$^1S_0$	$^3P_0$	$^3P_1$	$^3P_2$	$^1D_2$
$^1S_0$	$E_0+12F^2/25$	$\sqrt{2}\zeta$	0	0	0
$^3P_0$	$\sqrt{2}\zeta$	$E_0-3F^2/25+\zeta$	0	0	0
$^3P_1$	0	0	$E_0-3F^2/25+\zeta/2$	0	0
$^3P_2$	0	0	0	$E_0-3F^2/25-\zeta/2$	$-\zeta/\sqrt{2}$
$^1D_2$	0	0	0	$-\zeta/\sqrt{2}$	$E_0+3F^2/25$

value given by the code $\zeta(2p^{-1})$ with the experimentally measured value ζ_{expt}:

$$\zeta_{\text{eff}}(2s^{-1}2p^{-1})=F\zeta_{\text{code}}(2s^{-1}2p^{-1})\,, \tag{3}$$

where

$$F=\zeta_{\text{expt}}/\zeta_{\text{code}}(2p^{-1})\,, \tag{4}$$

with corresponding corrections for the $(1s\,2p)^{-1}$ and $(2p)^{-2}$ configurations. In this way we have tried to make the results as accurate as possible within the framework of single-configuration, atomic, Hartree-Fock calculations. In addition, we have ignored any coupling between the hole states and the unfilled valence shells.

Table I shows the Hamiltonian for the relevant configurations in a L-S coupled basis, while Tables II and III give the appropriate dipole matrix elements. These were calculated using the standard techniques of Racah algebra as summarized by Cowan.[10] There are six satellite lines from the $(1s\,2s)^{-1}\rightarrow(2s\,2p)^{-1}$ transition which are dipole allowed in the intermediate-coupling approximation, while there are 14 from the $(1s\,2p)^{-1}\rightarrow(2p)^{-2}$ transition. These transitions are listed in Table III along with an identifying letter for each line and the relative intensity for pure L-S coupling. Although these intensities are modified considerably in the higher-Z elements, they are still useful as an indication of which lines are the brightest. As usual, the L-S coupling designation is used to identify intermediate coupled states even when there is considerable admixing.

TABLE II. Reduced dipole-matrix elements in L-S coupling. The entries have been divided by the radial dipole integral. (a) $(1s\,2s)^{-1}\rightarrow(2s\,2p)^{-1}$, (b) $(1s\,2p)^{-1}\rightarrow(2p)^{-2}$.

(a)

	$^1S_0$	$^3S_1$
$^1P_1$	1	0
$^3P_0$	0	$-1/\sqrt{3}$
$^3P_1$	0	1
$^3P_2$	0	$-\sqrt{5/3}$

(b)

	$^1P_1$	$^3P_1$	$^3P_0$	$^3P_2$
$^1S_0$	$-\sqrt{2/3}$	0	0	0
$^3P_0$	0	$-\sqrt{2/3}$	0	0
$^1D_2$	$-\sqrt{10/3}$	0	0	0
$^3P_2$	0	$\sqrt{5/6}$	0	$\sqrt{5/2}$
$^3P_1$	0	$\sqrt{1/2}$	$\sqrt{2/3}$	$-\sqrt{5/6}$

III. RESULTS

Figure 1 shows the results of our calculations for all elements from K to Ge ($19\leq Z\leq 32$). Intensities relative to the strongest line are plotted as a function of the energy separation from the $K\alpha_1$ energy in eV. The $(1s\,2s)^{-1}\rightarrow(2s\,2p)^{-1}$ complex, the $(1s\,2p)^{-1}\rightarrow(2p)^{-2}$ complex, and Parratt's experimental results are shown for each element.

Note that the strong line e^* ($^1S_0\rightarrow{}^1P_1$) is seen only on the graphs for Cu and Cr because its energy is usually so low that it is less energetic than the $K\alpha_1$ line. Cu and Cr are exceptions because their ground-state configurations are of the form $(3d)^n4s$ rather than the $(3d)^n(4s)^2$ of their neighbors. Pulling the $4s$ electron into the $3d$ shell increases the energy of the $(1s\,2s)^{-1}\rightarrow(2s\,2p)^{-1}$ complex relative to the other transitions thus bringing the line, e^*, to the high-energy side of the $K\alpha_1$ line.

One should also note that the calculated energies for titanium have been increased by 4 eV before plotting in order to facilitate a comparison between experimental and calculated line splittings. We do not understand why this was necessary for Ti and nor for any other element.

Two major conclusions can be drawn immediately from these graphs. First, α'', which Parratt finds for each ele-

TABLE III. Dipole transitions in intermediate coupling. The letters presented will be used to identify a particular transition. The intensities are for pure L-S coupling and may be greatly different in intermediate coupling for high-Z elements.

	Identifying letter	Transition	L-S Coupled relative intensity
$(1s\,2s)^{-1}\rightarrow(2s\,2p)^{-1}$	a^*	$^3S_1\rightarrow{}^3P_2$	1.0
	b^*	$^3S_1\rightarrow{}^3P_1$	0.6
	c^*	$^3S_1\rightarrow{}^3P_0$	0.2
	d^*	$^1S_0\rightarrow{}^3P_1$	0
	e^*	$^1S_0\rightarrow{}^1P_1$	0.6
	f^*	$^3S_1\rightarrow{}^1P_1$	0
$(1s\,2p)^{-1}\rightarrow(2p)^{-2}$	a	$^1P_1\rightarrow{}^1D_2$	1.0
	b	$^3P_2\rightarrow{}^3P_2$	0.75
	c	$^3P_1\rightarrow{}^3P_2$	0.25
	d	$^3P_2\rightarrow{}^3P_1$	0.25
	e	$^1P_1\rightarrow{}^1S_0$	0.20
	f	$^3P_0\rightarrow{}^3P_1$	0.20
	g	$^3P_1\rightarrow{}^3P_0$	0.20
	h	$^3P_1\rightarrow{}^3P_1$	0.15
	i	$^3P_2\rightarrow{}^1D_2$	0
	j	$^3P_1\rightarrow{}^1D_2$	0
	k	$^1P_1\rightarrow{}^3P_1$	0
	l	$^1P_1\rightarrow{}^3P_2$	0
	m	$^1P_1\rightarrow{}^3P_0$	0

ment from potassium to vanadium, cannot be explained by any transition involving single spectator holes in the L shell. These transitions have no lines with energy near the α'' energy. In particular, the assignment of the $^1S_0\rightarrow{}^1P_1$ transition from the $(1s\,2s)^{-1}\rightarrow(2s\,2p)^{-1}$ complex to α'' as indicated by Nigam and Kothari[7] and by Horák[6] is untenable.[11]

Second, there is no evidence that the $(1s\,2s)^{-1}\rightarrow(2s\,2p)^{-1}$ complex contributes significantly to the satellites. This is especially clear for Cr and Cu where a^* (the strongest line of the complex) lies in a region where there are no competing strong lines from the $2p$ spectator-hole transition. In neither case did Parratt observe a line. We conclude that the $2s$ spectator-hole contribution is negligible. This is probably due to Coster-Kronig transitions which rapidly fill the $2s$ hole thus greatly reducing the probability for radiative transitions out of this state.

By comparing the spectrum of the $(1s\,2p)^{-1}\rightarrow(2p)^{-2}$ complex with Parratt's results we can assign specific transitions to each experimental line. These assignments are shown in Table IV and, taken as a whole, provide convincing detailed evidence for assigning the satellite lines to a transition involving a single $2p$ spectator hole. It should be noted that extracting intensities and energies of the weakest lines (α' and α_3'') from the experimental data is a difficult task filled with ambiguities. Thus the experimental intensities should be considered as qualitative indicators only. In this light, the agreement between our calculations and Parratt's experimental results is remarkably good.

α_4. Line a is the major component of α_4 in all cases. As one considers elements with decreasing atomic number, one notes that the line f, begins at Ge with higher energy than line a but progressively moves to lower relative energy until at V it may be associated with α_3 or α_3' rather than α_4. This transition region is somewhat arbitrary, but we have made the assignments shown in Table IV with the knowledge that the experimental determination of the energies of α_3, α_4, α_3', α_3'', and α' is always somewhat uncertain where all of the lines are not experimentally resolved.

α_3. Line b is the major component of α_3 in all cases, but as Z decreases, lines g and h come so close to b that they contribute as well.

α_3'. Line c is the major component of α_3' in all cases, but for the low-Z elements, f also contributes.

α' and α_3''. These are the weakest of the satellite lines and the most complex to explain. For Ge and Ga α_3'' is not present and α' is clearly line g. For Zn and Cu, however, line h has moved close enough to g so that Parratt, unable to resolve them, places α' between the two. At Ni, g and h are resolved into α' and α_3''. Unfortunately, the nomenclature is confused so that the lower energy line is called α' whereas the line associated with g is now called α_3''. As we consider lower-Z atoms, line d moves farther away from $K\alpha_1$ and h moves closer to g, until at Mn we identify α_3'' with both g and h. This migration of lines continues for one more cycle until at K, α_3'' is identified with line d. The fact that α' is often placed between two lines reflects the inability of Parratt to resolve two weak lines in the presence of stronger lines. This is especially clear in the transition from Cu to Ni where α_3'' makes its first resolved appearance. It is a great tribute to Parratt's skill and insight that he was able to resolve so many of

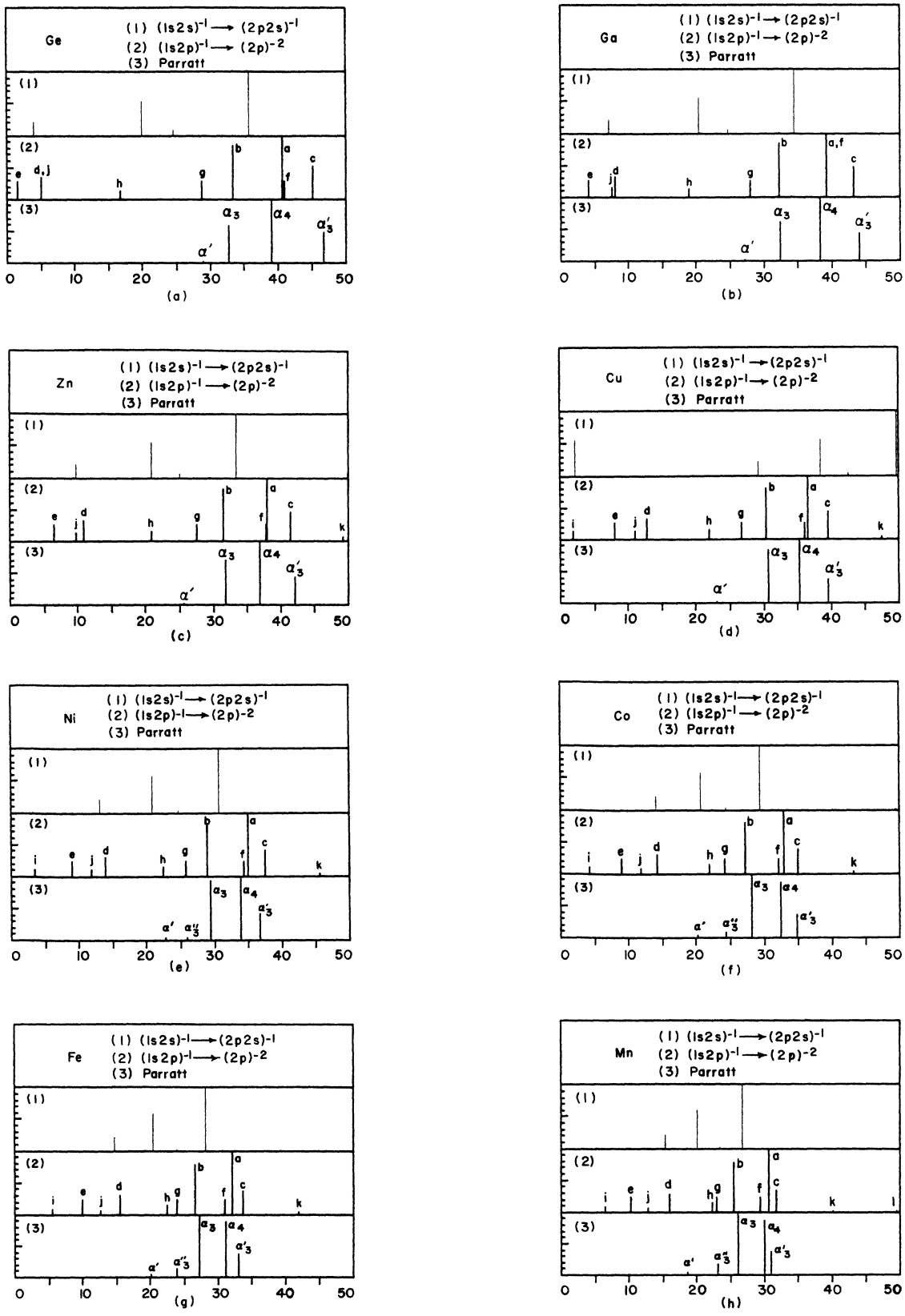

FIG. 1. Intensities relative to the strongest line as a function of the displacement (in eV) from the $K\alpha_1$ line for all elements having atomic numbers from 19 to 32 (K to Ge). In each graph the bottom set of lines shows Parratt's experimental data, the middle set gives our results for the $(1s\,2p)^{-1} \rightarrow (2p)^{-2}$ complex, while the top set gives our results for the $(1s\,2s)^{-1} \rightarrow (2s\,2p)^{-1}$ complex. Intensity normalization among the three sets is arbitrary.

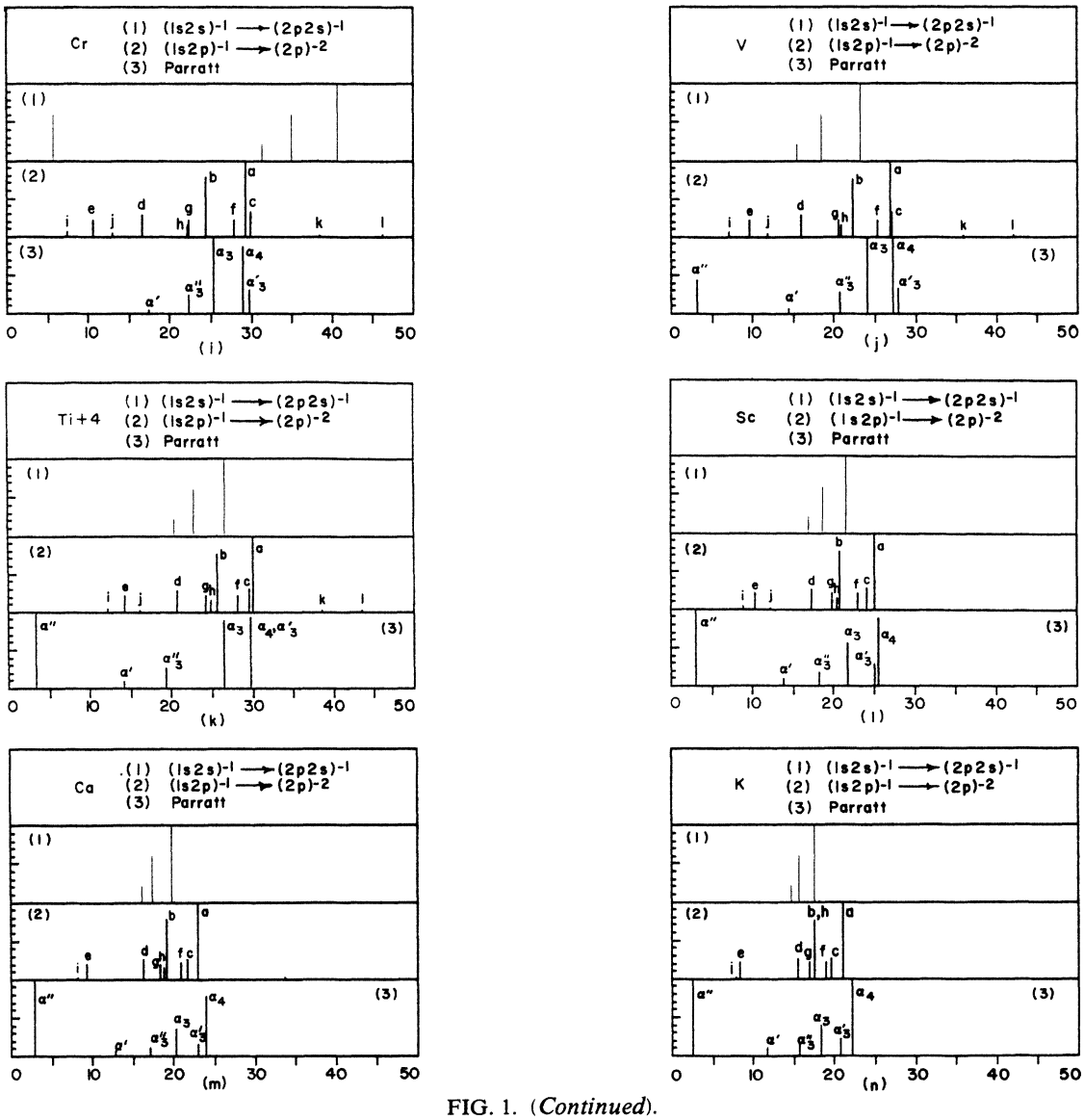

FIG. 1. (*Continued*).

TABLE IV. $K\alpha$ satellite transition assignments. See Table III for letter definitions. All lines are from the $2p$ spectator-hole complex: $(1s\,2p)^{-1}\rightarrow(2p)^{-2}$. A dash indicates that there is no experimental data for that entry.

	Line assignment				
Element	α_4	α_3	α_3'	α'	α_3''
Ge	*a,f*	*b*	*c*	*g*	—
Ga	*a,f*	*b*	*c*	*g*	—
Zn	*a,f*	*b*	*c*	*g*	—
Cu	*a,f*	*b*	*c*	*h,g*	—
Ni	*a,f*	*b*	*c*	*h*	*g*
Co	*a,f*	*b*	*c*	*h*	*g*
Fe	*a,f*	*b*	*c*	*h*	*g*
Mn	*a,f*	*b*	*c*	*d*	*g,h*
Cr	*a,f*	*b*	*c*	*d*	*g,h*
V	*a*	*b,f*	*c*	*d*	*g,h*
Ti	*a*	*b,g,h*	*c,f*	*e*	*d*
Sc	*a*	*b,g,h*	*c,f*	*e*	*d*
Ca	*a*	*b,g,h*	*c,f*	*e*	*d*
K	*a*	*b,g,h*	*c,f*	*e*	*d*

these weak lines so accurately many years before the birth of electronic computers.

It is clear from Table IV that α' and α_3'' have no single explanation. They result from different terms of the complicated multiplet structure and their components vary from atom to atom.

IV. DISCUSSION

The correct explanation of the $K\alpha$ satellite lines as arising from $K^{-1}L^{-1}\rightarrow L^{-2}$ transitions was first given many years ago, but detailed assignments had been unsatisfactory. Nigam and Kothari[7] correctly gave the major components of α_4, α_3, and α' (as did Horák[6] and Kennard and Ramberg[3]) but mistakenly assigned α_3' to the $2s$ spectator-hole transitions a^*, b^*, and c^* and had to invoke L-S forbidden transitions i and j to explain α_3''. This misassignment resulted from using the neutral-atom calculations of Gianturco, Semprini, and Stefani.[4]

Neutral-atom calculations are greatly in error for the $(1s\,2s)^{-1}$ state for reasons closely related to Koopmans[12]

theorem. For filled S shells, as in the neutral atoms, the off-diagonal energy parameter in the Hartree-Fock equations is set to zero, whereas for the $(1s\,2s)^{-1}$ state this parameter is allowed to vary. For iron, this changes the Slater integral $G^0(1s\,2s)$ from the neutral-atom value of 11.8 eV to the $(1s\,2s)^{-1}$ value of 1.8 eV so the $^3S_1$-$^1S_0$ splitting decreases from 23.6 to 3.6 eV. This has the effect of placing the line e^* at lower energy than $K\alpha_1$ and removes it from consideration as an explanation for α''. Similarly, α_3' cannot be understood as a $2s$ spectator-hole transition, but rather, it is a $2p$ spectator-hole transition.

It is difficult to assess the accuracy of our calculations. We believe that most of the significant relativistic effects are accounted for by using experimental values for the $K\alpha$ energies and the spin-orbit parameter $\zeta(2p^{-1})$. A relativistic Dirac-Fock calculation performed by Hodge[13] gave 6427 eV as the configuration average transition energy for the $(1s2p)^{-1}\rightarrow(2p)^{-2}$ transition in iron. Our calculations gave the same result. In order to assess the importance of chemical effects and the neglect of coupling with the unfilled valence shell, we repeated the calculations for iron with one electron removed from the $4s$ shell (in addition to those already missing for the transition being considered). In no case did the results change by as much as 0.1 eV. We conclude that these effects are negligible here.

Taking this into account and considering the overall results as displayed in Fig. 1, we believe that our calculations are accurate to 1 or 2 eV absolutely and substantially better with regards to the splitting. This conclusion must be tempered by the fact that a 4-eV shift in computed energies was needed to bring the values for Ti into agreement with experiment. We do not understand the reason for this.

ACKNOWLEDGMENTS

One of us (B.L.S.) would like to thank the California State University for financial support. We also wish to thank Dr. Sema'an I. Salem for many helpful discussions.

[1]L. G. Parratt, Phys. Rev. **50**, 1 (1936).
[2]M. J. Druyvesteyn, Z. Phys. **43**, 707 (1927).
[3]E. H. Kennard and E. Ramberg, Phys. Rev. **46**, 1040 (1934).
[4]F. A. Gianturco, E. Semprini, and F. Stefani, Physica **80C**, 613 (1975).
[5]V. P. Sachenko and V. F. Demekhin, Zh. Eksp. Teor. Fiz. **49**, 765 (1965) [Sov. Phys.—JETP **22**, 532 (1966)].
[6]Z. Horák, Proc. Phys. Soc. London Sec. A **77**, 980 (1961).
[7]A. N. Nigam and S. Kothari, Phys. Rev. A **21**, 1256 (1980).
[8]C. Froese Fischer, Comput. Phys. Commun. **4**, 107 (1972).
[9]J. A. Bearden and A. F. Burr, Rev. Mod. Phys. **39**, 125 (1967).
[10]R. D. Cowan, *The Theory of Atomic Structure and Spectra* (University of California Press, Los Angeles, 1981).
[11]Preliminary calculations on vanadium indicate that α'' can be understood as a $(1s\,3p)^{-1}\rightarrow(2p\,3p)^{-1}$ transition.
[12]T. A. Koopmans, Physica **1**, 104 (1933). See also C. Froese Fischer, *The Hartree-Fock Method for Atoms* (Wiley, New York, 1977).
[13]B. Hodge, private communication, as reported in Ref. 7.